Surface Quasielastic Light Scattering from Spread Films of Cyclic Poly(ethylene oxide)

C. Booth,[‡] R. W. Richards,*[,†] M. R. Taylor,[†] and G.-E. Yu[‡]

Interdisciplinary Research Centre in Polymer Science and Technology, University of Durham, Durham DH1 3LE, UK, and Department of Chemistry, University of Manchester, Manchester M13 9PL, UK

Received: October 28, 1997; In Final Form: December 31, 1997

We report the use of surface quasi-elastic light scattering (SQELS) to investigate the dynamic surface properties of spread films of cyclic poly(ethylene oxide) at various surface concentrations of polymer. Application of an unbiased phenomenological fitting function to the collected heterodyne correlation functions allows the frequency and damping of the capillary waves to be measured. Increasing the surface concentration of polymer causes complex variations in the capillary wave frequency and damping which can only be explained by the existence of a resonance between the capillary and dilational waves. We further analyze the correlation functions in terms of four surface viscoelastic parameters—surface tension, transverse shear viscosity, dilational modulus, and dilational viscosity—via a direct "spectral fit" to the data. At surface concentrations where the surface is saturated with polymer, at least one relaxation process occurs in the frequency regime studied. For the dilational mode of the interface, this relaxation is associated with the rate of desorption of polymer chains from the interface into the subphase when the surface is saturated with polymer. Both viscosities have unusual properties—the transverse shear viscosity decreases at intermediate surface concentrations before increasing again with surface concentration, and the dilational viscosity is always negative. This apparently unphysical measurement may have two origins: either a coupling with another surface oscillation mode or, because the dispersion equation does not describe the surface behavior completely, an idea supported by the discrepancy between the capillary wave dampings calculated from the observed surface viscoelastic parameters and those measured directly.

Introduction

Polymers at interfaces have been the subject of much study, both theoretically and experimentally, of late. Linear polymers at surfaces have been described as occurring in states labeled as "pancakes", "mushrooms", and "brushes".[1] The brushlike region has been the focus of most activity, and the predictions of the variation of brush height with surface density of polymer have been well confirmed by experiment, the premier technique used being neutron reflectometry. Our knowledge and understanding of the dynamics of polymer layers at interfaces does not, however, match the wealth of theory and data about their equilibrium organization. For a fluid interface—liquid−liquid or liquid−air—there are few ways of studying the dynamics without severe perturbation of the interface, and our theoretical understanding is limited. One way to investigate the dynamics of polymers at fluid interfaces is through their effect on and interaction with the capillary waves at the interface.[2] Capillary waves are thermally induced surface motions which continually roughen a fluid interface. The motion of these waves stresses the polymer film, although at this stage we make no assumptions as to its response to this stress; it could be purely viscous, purely elastic, or viscoelastic. A number of different surface stress modes are possible,[3,4] but only two are relevant here: shear transverse to the surface and compression/dilation in the plane of the surface. The surface parameters of interest are the surface tension (γ_0) and the Gibbs elasticity or dilational modulus (ϵ_0). These two parameters have associated viscosities: the transverse shear viscosity (γ') and the dilational viscosity (ϵ'). An experimental technique that is able to measure the frequency spectrum of the capillary waves will be sensitive to these viscoelastic moduli and in principle afford a means for their evaluation.

Since capillary waves are known to scatter light, the techniques of photon correlation spectroscopy have been applied in order to study them:[2] the technique has become known as surface quasi-elastic light scattering (SQELS), sometimes shortened to just surface light scattering. (We prefer the former title since it emphasizes the frequency dependence of the scattering process.) As the technique has advanced, it has been applied to a wide variety of systems: pure liquids, surfactant solutions, membranes, and more recently polymers.[2] At the same time, SQELS instrumentation and instrumental methods have improved, major advances being the reliable provision of a local oscillator (for heterodyning),[5] correct allowance for the line width and other instrumental factors,[6] multiphoton counting,[7] and full unbiased fitting to the complete spectrum of scattered light.[8] Recently, a design for a combined bulk−surface light scattering instrument was published.[9]

Poly(ethylene oxide) (PEO) is a technically important and academically intriguing polymer. Soluble in water, it spontaneously forms an adsorbed film at the air−solution interface, i.e., a surface excess layer, because of its much lower surface tension relative to that of water.[10] However, despite its solubility, it can also form a stable spread film at the air−water interface.[11,12] The surface properties of linear PEO and copolymers containing PEO have been studied extensively,[11−20] although different workers have studied different aspects of the systems. Relevant to the present work is a previous study from this laboratory on

* To whom correspondence should be addressed.
[†] University of Durham.
[‡] University of Manchester.

S1089-5647(98)00008-X CCC: $15.00
Published on Web 02/25/1998

linear PEO spread films at a range of surface concentrations,[12] where we observed startling changes in surface properties above surface concentrations of 0.5 mg m^{-2} of spread polymer. Neutron reflectometry studies[11] have shown that at this surface concentration the linear PEO chains begin to penetrate significantly into the subphase. Cyclic ethylene oxide polymers of various molecular weights have been synthesized recently.[21,22] One might anticipate differences in the behavior of the otherwise chemically identical linear and cyclic PEO because of the lack of free ends in the cyclic polymer. Certainly the static scattering functions for the linear and cyclic polymer molecules differ.

In this paper we present the first survey of the surface behavior of a spread cyclic poly(ethylene oxide) film. First we give a brief review of the relevant SQELS theory and the apparatus. A presentation of the measured frequencies and dampings of capillary waves as a function of surface concentration of polymer at a fixed q, the scattering vector, follows. One surface concentration, 0.4 mg m^{-2}, is then chosen, and the frequency and damping are determined as a function of the scattering wavevector q. Further, we take advantage of recent developments in the analysis of SQELS data[8] to extract surface viscoelastic parameters at various surface concentrations and capillary wave frequencies directly from the correlation functions of the scattered light. Finally, a comparison is made between the surface behavior of the cyclic polymer studied here and previous measurements on linear PEO.

Theory

An excellent introduction to capillary waves and the use of SQELS to quantify them has been published elsewhere,[2] and we will not attempt to reproduce the description; however, a précis of the relevant theory is useful to help understanding the results presented here. In the absence of external mechanical disturbance a fluid−fluid interface is still rough on a microscopic scale due to thermal motions of its constituent atoms or molecules. The best available description of these motions Fourier decomposes them into capillary waves. Capillary waves have a small amplitude (∼angstroms): the amplitude is temperature and interfacial tension dependent and thus can increase dramatically near critical points. Generally for SQELS accessible capillary waves the wavelength ($=2\pi/q$ where q is the capillary wavenumber) is of the order of 100 μm, and the associated frequency is of the order of 10^5 Hz. When an interfacial film is present whose elastic properties differ from the two media either side, longitudinal (in-plane) fluctuations exist which can be decomposed into dilational waves. A coupling exists between these dilational and the capillary waves. In this experiment we are primarily interested in the capillary waves since these are the surface fluctuations which are detected by light scattering; however, the dilational waves do have an indirect effect on the scattered light, via this coupling, as we will discuss later.

The propagation of the capillary and dilational waves is described by a dispersion relation, $D(\omega)$, which for the present case—a monolayer spread at an air−water interface—has the form

$$D(\omega) = [\eta(q-m)]^2 - \left\{\frac{\epsilon}{\omega}q^2 + \mathrm{i}[\eta(q+m)]\right\} \times \left\{\frac{\gamma}{\omega}q^2 - \frac{\omega\rho}{q} + \mathrm{i}[\eta(q+m)]\right\} \quad (1)$$

where $m = (q^2 + \mathrm{i}\omega\rho/\eta)^{1/2}$ and $D(\omega) = 0$ for a solution to the equation.

In the experiment described below, measurements are made at a fixed, real scattering vector q. The surface waves propagate but are underdamped so the frequency ω is complex: $\omega = \omega_0 + \mathrm{i}\Gamma$ where ω_0 is the real frequency and Γ the damping of the oscillatory solutions to the dispersion eq 1. As indicated above, there are two such solutions: capillary (transverse shear) waves and dilational waves. Only the capillary waves, however, scatter light appreciably. Moduli for the transverse shear and in-plane dilation of the surface are γ and ϵ, respectively; these are complex quantities which we expand on below. In (1) the subphase liquid viscosity is denoted η and ρ is the liquid density.

If there are no loss processes in the film (i.e., the capillary wave damping is entirely due to the viscosity of the subphase), then γ can be identified as the surface tension and ϵ the elasticity:

$$\epsilon = -\frac{\partial\gamma}{\partial \ln \Gamma_s} \quad (2)$$

where Γ_s is the surface concentration of material. For many polymer monolayers at the air−water interface dissipative effects additional to those due to the viscosity of the subphase are observed. These dissipative effects can be incorporated into the transverse shear and dilational moduli by expanding them as linear response functions[4]

$$\gamma = \gamma_0 + \mathrm{i}\omega\gamma' \quad (3a)$$

$$\epsilon = \epsilon_0 + \mathrm{i}\omega\epsilon' \quad (3b)$$

where γ_0 and ϵ_0 are the moduli for transverse shear and dilation of the surface, and the primed quantities are the associated viscosities. (NB: from here on the transverse shear modulus will be referred to by the more widely accepted form, surface tension.) The exact effect of the viscosities on the oscillations is complex, but approximately we can say that increasing the transverse shear viscosity increases the damping of the capillary waves and increasing the dilational viscosity increases the damping of the dilational waves. In this model of surface dynamics these four parameters determine completely the behavior of the waves on the surface.

For the case of a bare interface (i.e., no surface film present of nature different from the subphase), $\gamma = \gamma_{st}$ (the static surface tension), $\epsilon = 0$, and at low q the frequency and damping of the capillary waves can be described by two approximate solutions to the dispersion equation:

$$\omega_0 = q^3(\gamma/\rho)^{1/2} \quad (4a)$$

and

$$\Gamma = 2(\eta/\rho)q^2 \quad (4b)$$

Similarly the dilational waves have a low q approximation:

$$\omega_{D0} = \frac{\sqrt{3}}{2}\left(\frac{\epsilon^2 q^4}{\eta\rho}\right)^{1/3} \quad (5a)$$

and

$$\Gamma_D = \frac{1}{2}\left(\frac{\epsilon^2 q^4}{\eta\rho}\right)^{1/3} \quad (5b)$$

The dilational and capillary waves are coupled, and resonance effects are observed between the two waves. In Figure 1 we show a numerical solution to the dispersion equation (eq 1) for

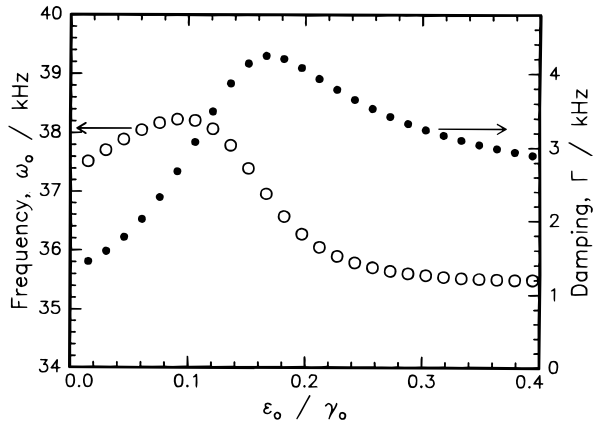

Figure 1. Predicted variation of frequency and damping of the capillary waves with the ratio ϵ_0/γ_0 for $\gamma_0 = 66$ mN m^{-1} and $\gamma' = \epsilon' = 0$ at $q = 277$ cm^{-1}, showing resonance at $\epsilon_0/\gamma_0 = 0.16$.

$q = 277$ cm^{-1}, with $\gamma_0 = 66$ mN m^{-1}, ϵ_0 varying from 0 to 26 mN m^{-1} and γ', $\epsilon' = 0$. There is a clear peak in the capillary wave damping at a ratio of dilational modulus to surface tension of 0.16. Earnshaw has pointed out that the two sets of waves can in fact be described as coupled damped oscillators, and he has described theoretically and experimentally the situations for observing mode mixing.[23,24]

The power spectrum of light scattered from the surface by the capillary waves is given by[25]

$$P(\omega) = -\left(\frac{k_B T}{\pi\omega}\right) \mathrm{Im}\left[\frac{i\omega\eta(q+m) + \epsilon q^2}{D(\omega)}\right] \qquad (6)$$

Since this expression for the spectrum contains the dispersion equation, it is possible to fit it to light scattering data in order to obtain all four surface viscoelastic parameters. Physically, although the light is scattered by the capillary waves only, because of the coupling between capillary and dilational waves it is possible to determine the dilational modulus and viscosity. The power spectrum is approximately a skewed Lorentzian (see, for example, Chapter 11 of ref 2), with a maximum that is the frequency of the capillary wave ω_0 and a width proportional to the capillary wave damping Γ. Recording the scattered light in the time domain and using heterodyne correlation methods results in the correlation function having the appearance of a damped cosine function, with a frequency ω_0 and a damping Γ.

Experimental Section

Polymer. The synthesis of the cyclic poly(ethylene oxide), cPEO, used here has been described elsewhere.[26,27] The ring closure was via an acetal linkage. Characterization of the polymer by NMR gave $M_n = 10\,000$ g mol^{-1}, and SEC gave a polydispersity of 1.1.[26] Further measurements[26] in solution by PGSE-NMR (self-diffusion coefficient) and in the solid state[27] by X-ray scattering (lamellar spacing) and Raman spectroscopy (LAM-1 frequency) have served to confirm its cyclic structure and average molar mass.

Surface Quasielastic Light Scattering. The SQELS apparatus has been previously described;[12] only brief details will be given here. Polarized light from a diode-pumped YAG laser (100 mW CW, 532 nm) was focused on the water surface: the reflected and scattered light were collected by a mirror and directed toward a photomultiplier tube (PMT). Scattered light was detected by heterodyne correlation, with the local oscillator being provided by an optical system of two lenses either side of a diffraction grating (10 μm lines separated by 150 μm) placed before the water surface. By this optical system the grating was imaged at the water surface, and then a series of reference light sources for heterodyne correlation were focused at the PMT. In a measurement one particular beam from the grating is selected, and this forms the reference beam for the light scattered from the main (undiffracted) beam at the same angle. By aligning on different beams, the scattering angle is varied, and thus capillary waves of different q and frequency can be accessed. The reference beam intensity was adjusted with neutral density filters to be between 10^3 and 10^6 times greater than that of the scattered light. The PMT output was processed by a standard Malvern amplifier−discriminator package, and the resultant pulses were collected by a 128-channel correlator.[28] A real-time output from the correlator to an oscilloscope allowed the quality of the correlation function being collected to be assessed. After collection, data were downloaded to a PC for storage and analysis. cPEO was investigated as a thin film spread from 1 mg/mL solutions in CH_2Cl_2 onto the surface of doubly distilled and deionized (resistivity 18 MΩ/cm^2) water. The water was contained in a Langmuir style PTFE trough,[29] with full computer control of the barriers and automatic recording of the surface pressure using a Wilhelmy plate suspended from a microbalance. This system allowed classical surface pressure−surface concentration isotherms to be recorded or specific surface pressures or surface concentrations of the polymer film to be set for examination by SQELS. The trough was mounted on a computer-controlled vibration isolation table, with the whole apparatus being mounted on a massive enclosed optical table, excluding dust, air currents, and laboratory vibrations. The temperature of the water in the trough was maintained at 293 K by a thermostat that circulated water through a labyrinth of channels immediately below the base of the PTFE trough.

Precise measurement of q is essential for accurate determinations of the surface viscoelastic parameters via the "spectral fitting" procedure (see below). It is possible to determine q from measuring the scattering angle δ and the incident angle θ, since

$$q = \frac{4\pi}{\lambda} \cos(\theta) \sin\left(\frac{\delta}{2}\right) \qquad (7)$$

However, we have found it more convenient to calibrate using a bare water surface—recording the correlation function at a certain reference spot and then spreading the cPEO film on the water surface.

Results

Two separate analyses were applied to the data. The first fits a model function to the data, to extract values for the frequency and damping of the capillary waves. These values can then be related *approximately* to the surface viscoelastic parameters. The second fitting method has been termed "spectral fitting", since it attempts to fit the Fourier transform of a theoretical power spectrum (derived from estimates of the parameters of the dispersion equation which described the capillary waves) to the experimental correlation function by adjusting the values of γ_0, γ', ϵ_0, γ_0, γ', ϵ_0, and ϵ'.

Frequency and Damping. The experimentally measured correlation function (Figure 2) clearly has the appearance of a damped cosine: similarly in the frequency domain the spectrum of scattered light is *approximately* Lorentzian in form. Thus, by fitting the equation of a damped cosine function, the frequency and damping of the capillary waves can be obtained.

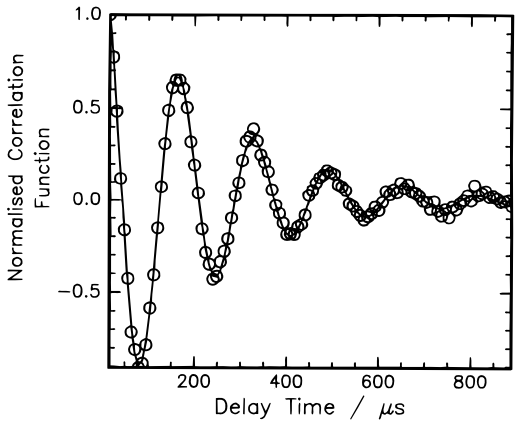

Figure 2. Normalized heterodyne correlation function of light scattered by capillary waves on water covered with a spread film of cPEO: $\Gamma_s = 0.3$ mg m^{-2}, $q = 277$ cm^{-1}; (○) data, (—) fit.

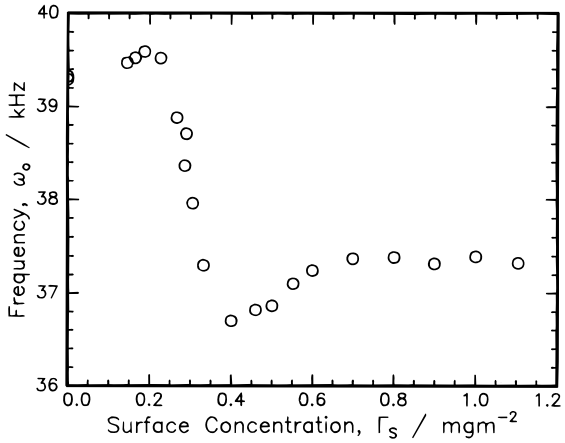

Figure 3. Variation in capillary wave frequency with surface concentration at $q = 277$ cm^{-1}. Errors on frequency determination are less than size of symbols.

The exact form of the equation used is[6]

$$g(\tau) = B - D\tau^2 + AF(\omega)\exp(-\beta^2\tau^2/4) \qquad (8)$$

with $F(\omega) = \cos(\omega_0 + \varphi)\exp(-\Gamma\tau)$. τ is the correlator delay time, A is the function amplitude, ω_0 and Γ are the frequency and damping of the capillary waves, and φ a phase term that accounts for the deviation of the frequency spectrum of scattered light from a Lorentzian form.[30] The background level, B, is modified by the term $D\tau^2$ to account for "droop" on the correlation function caused by any external mechanical vibrations. An extra damping term, of decay constant β^2, is introduced to account for the finite instrument resolution.[5]

Correlation functions of the light scattered from the air-water interface were first collected at a fixed scattering angle with a q value of 277 cm^{-1}, and the surface concentration of the spread film of cPEO was varied. Subsequently, a surface concentration of 0.4 mg m^{-2} was selected, and data were collected as a function of q. The results at fixed q, varying surface concentration, will be presented first, and then at fixed surface concentrations, varying q.

The variations of capillary wave frequency and damping with surface concentration at $q = 277$ cm^{-1} are shown in Figures 3 and 4. Initially at very low surface concentrations the frequency shows a slight increase above the value for a bare water surface, before decreasing to a minimum at 0.4 mg m^{-2} and then rising slightly. Above 0.7 mg m^{-2} the frequency shows no change on further compression of the film. Dramatic changes are also

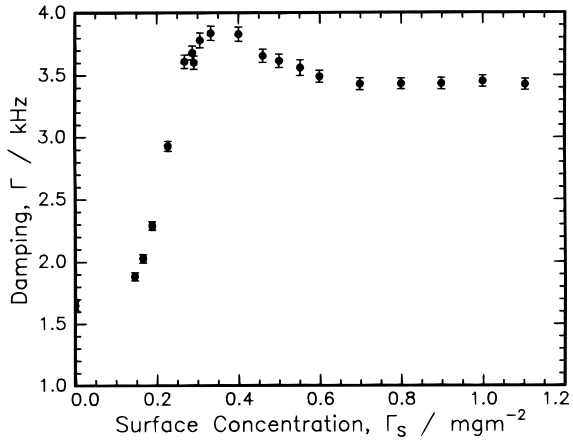

Figure 4. Variation in capillary wave damping with surface concentration at $q = 277$ cm^{-1}.

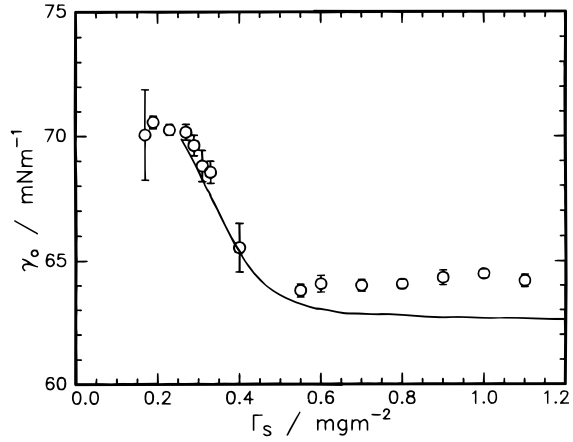

Figure 5. Surface tension as a function of surface concentration: (○) SQELS values at $q = 277$ cm^{-1}; (—) Wilhelmy plate values.

observed in the capillary wave damping as the surface concentration in increased. At low concentrations the wave damping rises to a maximum value at 0.4 mg m^{-2}, before declining slightly to a constant value above 0.7 mg m^{-2}.

A simple consideration based on the static surface pressure isotherm for cPEO (see Figure 5, solid line) and eq 4a predicts a monotonic decrease in the frequency as the concentration increases, up to 0.7 mg m^{-2}. Although this explains the overall drop in frequency, it does not explain the observed maximum and minimum. Clearly the behavior is more complex, and a fuller analysis of the data, using the dispersion equation of the capillary waves at the interface, is required as described below. The maximum seen in the damping is characteristic of the resonance (see below) between the observed capillary waves and dilational waves.[31]

The q dependence of the capillary wave frequency and damping for one surface concentration, 0.4 mg m^{-2}, is given in Figure 6 together with the predicted values for the air-water interface obtained by solving eq 1 with $\gamma_0 = 72$mN m^{-1} and γ', ϵ_0, and $\epsilon = 0$. Both the frequency and damping have the expected dependency on q, scaling as $q^{3/2}$ and q^2, respectively. The absolute values for frequency are approximately 5% lower than those for bare water at all q measured, due in part to the surface tension being lowered by the monolayer. The absolute values for the damping of the monolayer are over twice those of the bare water surface. Generally for surface films this extra damping is due to dilational viscosity, transverse shear viscosity, and the resonance between the capillary and dilational waves, either individually or in concert.[2] A fuller analysis of the data

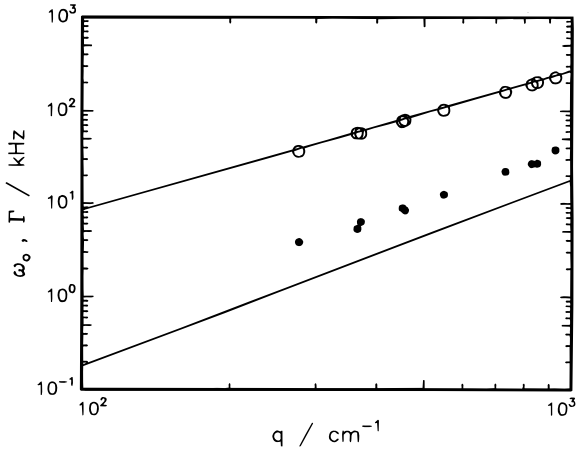

Figure 6. Dispersion of capillary waves with q for a spread film of cPEO at 0.4 mg m^{-2}: (○) measured ω_0, (●) measured Γ, (—) predictions for a bare water interface. Errors on data within size of symbols.

in terms of the viscoelastic parameters is required to decide the exact source of this extra damping.

Viscoelastic Parameters. Some authors have attempted to use the fitted frequency and damping values to obtain surface viscoelastic parameters. This can only be done by making certain assumptions—usually the identification of the SQELS measured surface tension with the static value (as measured by Wilhelmy plate methods for example) and a zero transverse shear viscosity. However, it has been clearly demonstrated that for SQELS from an air−water interface the four parameters surface tension, transverse shear viscosity, dilational modulus, and dilational viscosity influence the measured correlation function independently of each other and can be extracted from light scattering data by a second fitting method termed "spectral fitting".[8] This method attempts to fit the Fourier transform of the theoretical power spectrum (see eq 6), derived from estimates of the parameters of the dispersion equation, to the experimental correlation function. A function of the form of eq 8 is the model used, with $F(\omega)$ now the Fourier transformed power spectrum. The strength of the method is that no prior assumptions concerning values of any parameters need to be made. Its weakness, however, is that if the model dispersion equation is an incomplete description of the hydrodynamic properties of the surface region, the fit may return *effective* parameters. In the present case the necessity of using all four viscoelastic parameters to fit the data was confirmed by initially fitting the data with the transverse shear viscosity fixed to zero. The fits obtained were always of poorer quality (as measured by the correlation coefficient of the residuals) than those fitted using all four parameters.

The results of the direct fitting procedure at various surface concentrations and a fixed q of 277 cm^{-1} are shown in Figures 5 and 7−9. The surface tension as measured by SQELS decreases from that of water (72 mN m^{-1}) for the lowest surface concentration measured and continues to decrease as the surface concentration increases up to approximately 0.6 mg m^{-2}. Above this surface concentration the surface tension is constant at 64 mN m^{-1}. For comparison, the static surface tension as determined by Wilhelmy plate is also plotted. Below 0.4 mg m^{-2} the agreement between the two methods is close; however, above this surface concentration the dynamic SQELS-determined surface tension is consistently 1.5 mN m^{-1} higher than the static Wilhelmy plate determination.

The transverse shear viscosity is zero for a bare water surface;[32] for the lowest surface concentration studied here, 0.17 mg m^{-2}, it is 7×10^{-5} mN s m^{-1}. As the surface concentration increases, the transverse shear viscosity falls to a minimum of less than 2×10^{-5} mN s m^{-1} at 0.4 mg m^{-2} before increasing again.

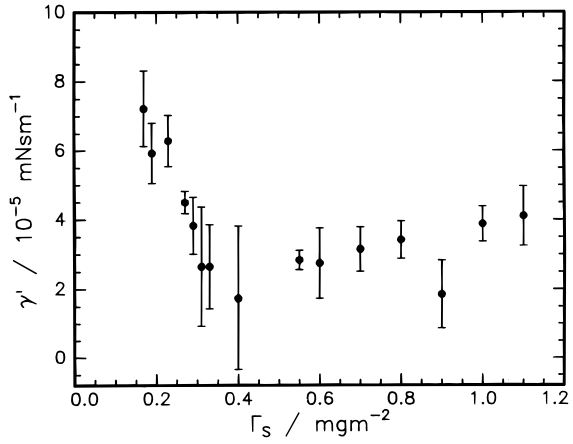

Figure 7. Transverse shear viscosity as a function of surface concentration at $q = 277$ cm^{-1}.

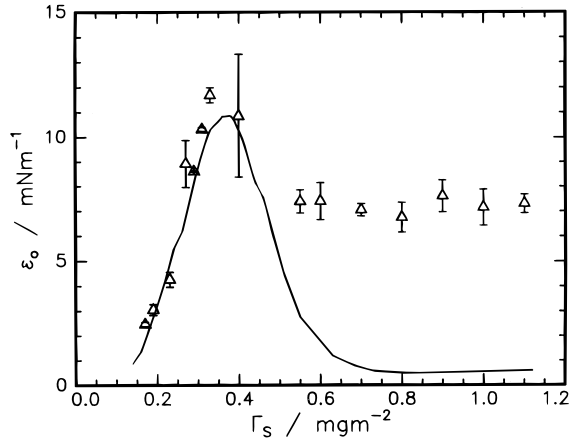

Figure 8. Dilational modulus as a function of surface concentration: (△) SQELS at $q = 277$ cm^{-1}; (—) static elasticity derived from Wilhelmy plate measurements.

Figure 8 shows the variation of dilational modulus with surface concentration and the equivalent static value (from the differentiated Wilhelmy plate data). The dilational modulus increases with the surface concentration, peaking at 0.3 mg m^{-2} and then falling. As with the surface tension data, below 0.4 mg m^{-2} there are only small differences between the static and dynamic (SQELS) measurements. Above this surface concentration, however, the static dilational modulus declines to nearly zero, whereas the dynamic value is constant, allowing for errors, at 7.5 mN m^{-1}. The associated dilational viscosity is, like the transverse shear viscosity, presumed to be zero for a bare water surface. The fitted values of dilational viscosity (Figure 9) are negative for all surface concentrations examined: increasing from 6×10^{-5} mN s m^{-1} at 0.17 mg m^{-2} to 1×10^{-5} mN s m^{-1} at 0.4 mg m^{-2}. Above this surface concentration the dilational viscosity is, within errors, constant at −10 nN s m^{-1}.

By varying the q at fixed surface concentrations of polymer the response of the surface to different capillary wave frequencies has been investigated. In this manner we have studied a surface concentration of 0.4 mg m^{-2}. The variations of surface tension, transverse shear viscosity, dilational modulus, and dilational viscosity with capillary wave frequency are presented for this surface concentrations in Figure 10a−d.

The surface tensions measured at 0.4 mg m^{-2} (Figure 10a)

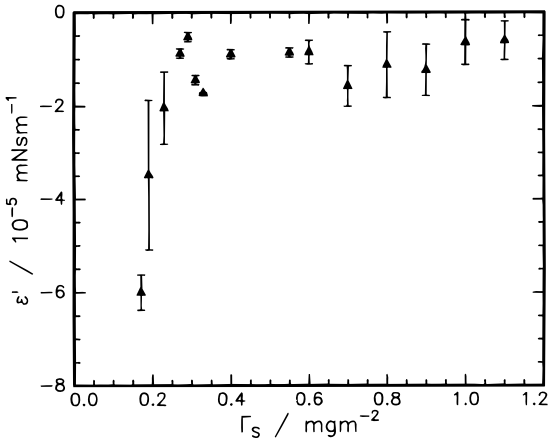

Figure 9. Dilational viscosity as a function of surface concentration at $q = 277$ cm^{-1}.

all fall within a 2 mN m^{-1} band around 66 mN m^{-1} with a small increase in the surface tension at the highest frequencies. This increase is only just larger than the scatter on the data so it is difficult to say whether this is a real trend or not. The transverse shear viscosities (Figure 10b) show a broad increase with frequency to about 100 kHz and then fall, although given the high degree of scatter of the data this may not be a significant trend. For the dilational modulus (Figure 10c), most fitted values were around 10 mN m^{-1}; however, two higher frequency measurements gave dilational moduli of around 2 and 4 mN m^{-1}. The most striking feature of the dilational viscosity data (Figure 10d) is that it is negative at all but the highest frequencies studied.

Discussion

Capillary Wave Frequency and Damping. In Figure 1 we showed theoretically predicted variations in capillary wave frequency and damping with ϵ_0/γ_0 at fixed q for fixed values of the surface parameters: $\gamma_0 = 66$ mN m^{-1}, $\gamma' = 0$, $\epsilon_0 = 0-26$ mN m^{-1}, and $\epsilon = 0$. Although these calculations are for fixed values of the surface viscosities, whereas in reality γ' and ϵ' vary, we can use Figure 1 to understand qualitatively the observed variations of frequency and damping of Figures 3 and 4. First consider how the ratio ϵ_0/γ_0 varies as the surface concentration varies: this is shown in Figure 11, using values derived from the Wilhelmy Plate measurements of the static surface tension and elasticity shown in Figures 5 and 8. As the surface concentration of polymer increases from 0, ϵ_0/γ_0 initially increases slowly and then above a surface concentration of around 0.2 mg m^{-2} increases somewhat more rapidly. The ratio ϵ_0/γ_0 continues to increase until $\Gamma_s = 0.38$ mg m^{-2} and then decreases rapidly to $\Gamma_s = 0.6$ mg m^{-2}. Above this surface concentration the ratio falls more slowly, approaching a constant value of about 0.01 which it reaches at around 0.8 mg m^{-2}.

The changing value of the ratio ϵ_0/γ_0 acts in conjunction with the changing absolute values of γ_0 and ϵ_0 in affecting the observed frequency and damping plotted in Figures 3 and 4. (The two surface viscosities, γ' and ϵ', will also have an effect, but for this initial qualitative analysis they can be ignored; we will discuss the viscosities in some depth later on.) As the surface concentration increases from 0 to 0.2 mg m^{-2}, the surface tension is approximately constant and the ratio ϵ_0/γ_0 increases, so the observed frequency increases slightly because of the small approach to the resonance condition of $\epsilon_0/\gamma_0 = 0.16$. Between 0.2 and 0.4 mg m^{-2} the ratio ϵ_0/γ_0 increases from 0.04 to 0.16, but only a small change in the capillary wave

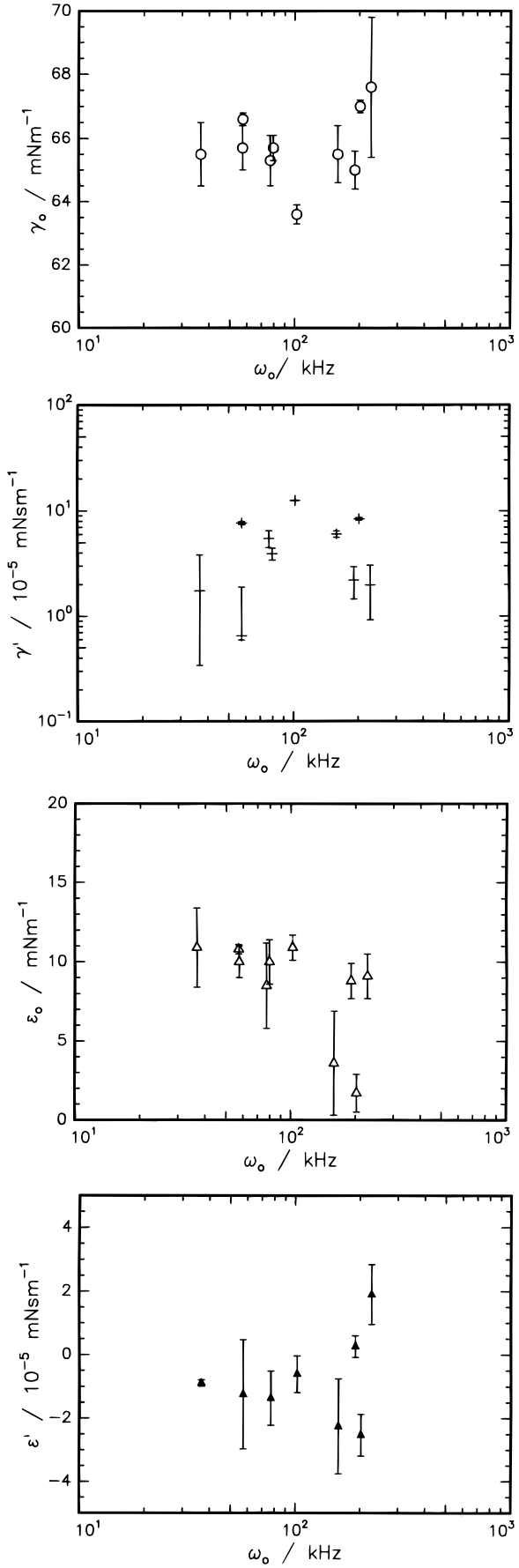

Figure 10. Surface viscoelastic parameters as a function of capillary wave frequency at a surface concentration of 0.4 mg m^{-2}, corresponding to resonance conditions: (a) surface tension, (b) transverse shear viscosity, (c) dilational modulus, (d) dilational viscosity.

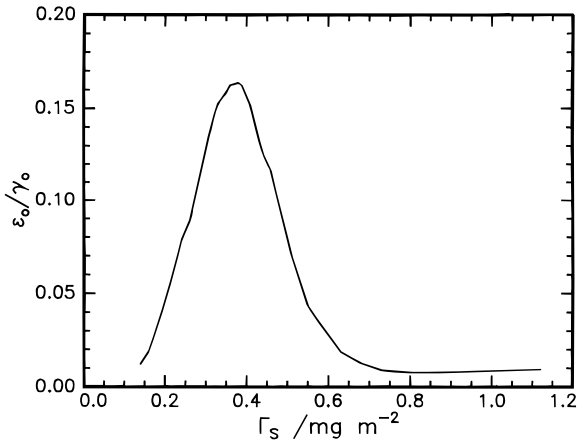

Figure 11. Variation of ϵ_0/γ_0 (measured by Wilhelmy plate) with surface concentration.

frequency is observed. The factor with greatest effect on the capillary waves in this surface concentration range is the surface tension which decreases significantly and thus causes the frequency to fall as would be expected from eq 4a. At higher surface concentrations, the surface tension is again approximately constant, but ϵ_0 falls in value drastically, and although ϵ_0/γ_0 decreases from 0.16, the reduction in damping due to the dilational modulus results in an increase in the frequency. Above 0.8 mg m^{-2}, both surface tension and dilational modulus are constant, and no further change in the frequency is observed.

The analysis of the damping variation with surface concentration is somewhat more straightforward. The damping increases monotonically as the surface concentration increases to about 0.4 mg m^{-2}. This is due to the resonance between the (observed) capillary waves and the (unobserved) dilational waves, which is maximal when $\epsilon_0/\gamma_0 = 0.16$, a condition which is reached at a surface concentration of 0.4 mg m^{-2}. Beyond this concentration the ratio decreases to a constant value of 0.1, and we observe a decrease to a constant value in the capillary wave damping.

Possible Structure of Layer. Before we discuss the values of the surface viscoelastic parameters measured in these experiments, it is worthwhile speculating on the structure of the spread cyclic polymer film. Unlike linear PEO, there is no structural information from neutron reflectometry available for this spread polymer system. We can, however, infer some structural information from the surface tension data given in Figure 5 by drawing comparisons with the well-documented surface tension behavior for linear PEO.[11] The surface tension isotherm for linear PEO shows a significant monotonic decrease of approximately 9 mN m^{-1} between 0.2 and 0.4 mg m^{-2} of spread polymer film and reaches a plateau surface tension around 9.5 mN m^{-1} below the bare water value above spread film concentrations of 0.6 mg m^{-2}. Structurally, in linear PEO, this plateau has been found to be associated with the surface "saturating" with polymer[11] at a surface concentration between 0.4 and 0.6 mg m^{-2}, and as the concentration increases above this value, the excess polymer goes into the subphase as loops or tails. The spread film of cyclic PEO which we have investigated here displays a similar isotherm behavior, with a plateau in the surface tension isotherm at around 0.6 mg m^{-2} and no evidence that the surface pressure subsequently increased on compression of the layer above 1.0 mg m^{-2}. It is likely therefore that above 0.6 mg m^{-2} the surface can contain no more cyclic polymer, and further compression of the film produces desorption of the polymer as loops into the subphase. One significant difference from the linear polymer is that the cyclic polymer will not have tails which penetrate the subphase to greater depths.

Transverse Surface Viscoelastic Parameters. We have shown that the variations in capillary wave frequency and damping with surface concentration can be qualitatively understood by the changing values of the surface viscoelastic parameters. But what are the causes of the changes in the surface viscoelastic parameters? At low surface concentrations (below 0.4 mg m^{-2}) the SQELS-measured values for surface tension are close to those measured statically using a Wilhelmy plate. Above 0.4 mg m^2, the static values are much less than the SQELS values, indicating that relaxation processes occur in the frequency range between the Wilhelmy plate (effectively $\omega_0 = 0$) and SQELS ($\omega_0 \sim 35$ kHz) measurement. Differences between surface tensions of monolayers measured statically and dynamically by SQELS have been observed before in polymer,[12−24] lipid,[33] and surfactant[34,35] systems and are generally accompanied by a finite and positive transverse shear viscosity. To explain the differences in surface tension, an analogy is drawn between the linear response function of eq 3a and the complex viscoelastic response function used in conventional bulk rheology.[34] In this case stress $= G^*(\omega)\cdot$strain, with

$$G^*(\omega) = G'(\omega) + iG''(\omega) \tag{9}$$

By comparison with eq 3a, $G'(\omega) \equiv \gamma_0$ and $G''(\omega) \equiv \omega\gamma'$, and the surface tension and transverse shear viscosity may be frequency dependent. One of the simplest relaxation models, the Maxwell fluid model, predicts the frequency variation of the surface tension and transverse shear viscosity due to a single relaxation of time constant τ in terms of a relaxation strength G and the equilibrium (static) surface tension γ_e:

$$\gamma_0 = \gamma_e + G\frac{\omega^2\tau^2}{1+\omega^2\tau^2} \tag{10}$$

and

$$\gamma' = G\frac{\tau}{1+\omega^2\tau^2} \tag{11}$$

The surface tension is thus predicted to increase from its equilibrium value, as the frequency increases, for systems with $G > 0$. In bulk polymer solutions a crossover from viscous to viscoelastic behavior is usually observed as the concentration is increased. Here we have an analogous situation: at low surface concentrations the surface tension is equal to the equilibrium value, and at higher surface concentrations the system becomes viscoelastic with a finite G, leading to a raised surface tension relative to the $\omega_0 = 0$ value.

Neither of the viscosities measured in this experiment is the usual in-plane shear viscosity which can be measured by other means[36] and which generally shows an increase with concentration of material at the surface. The transverse shear viscosity however does not show a simple increase with surface concentration in these measurements. Since the transverse shear viscosity of a bare water surface is zero,[32] we presume that there must be an increase from 0 to at least 7×10^{-5} mN s m^{-1} as the surface concentration of polymer increases from 0 to 0.2 mg m^{-2}. Such an increase in viscosity with surface concentration would be expected simply by drawing an analogy with the 3-D bulk solution case: as the bulk concentration of polymer increases, so does the (shear) viscosity of a (linear) polymer solution. Similarly for our case as the surface concentration of

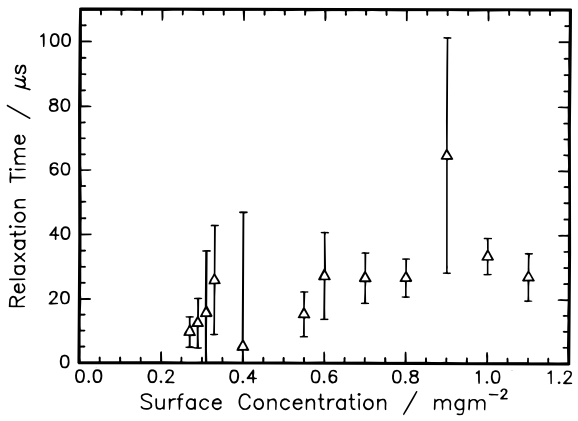

Figure 12. Transverse shear relaxation times at $\Gamma_s = 0.4$ mg m^{-2}.

polymer increases, so does the transverse shear viscosity. The fall in transverse shear viscosity between 0.2 and 0.4 mg m^{-2} cannot, however, be so easily rationalized. At 0.4 mg m^{-2} and above, as already noted, the PEO chains loop into the subphase. As the surface concentration increases, more of the polymer forms loops in the layer below the surface: the concentration of polymer in this layer now increases (with the concentration of polymer in the upper layer constant), and so again by analogy with the 3-D case we expect the viscosity to increase, as observed. In this surface concentration region the increasing penetration of the subphase is associated with the onset of relaxation as seen by the SQELS surface tension being higher than that measured by Wilhelmy plate.

The simplest realistic model of viscoelastic relaxation that has been shown to apply to spread polymer systems is the Maxwell model. By assuming that the relaxation is described by the Maxwell model, we can calculate the relaxation time at different surface concentrations for a fixed capillary wave frequency by combining eqs 10 and 11 to give

$$\tau = (\gamma_0 - \gamma_e)/\omega^2\gamma' \tag{12}$$

These times are plotted in Figure 12. Above 0.6 mg m^{-2} the relaxation time is constant at approximately 30 μs; below this the data have large error bars, but an increase from 0 to 30 μs is evident between 0.2 and 0.6 mg m^{-2}. Changes in relaxation time are associated with changes in the organization of the layer:[12,14] this corresponds well with the ideas expressed earlier about the surface organization.

Dilational Surface Viscoelastic Parameters. Below 0.4 mg m^{-2} the differences between the Gibbs elasticity ($= -\partial\gamma/\partial \ln \Gamma_s$) and dilational modulus values are negligible; however, above this surface concentration the modulus is about 7.5 mN m^{-1}, whereas the elasticity falls to less than 1 mN m^{-1}. The elasticity, although referred to as an "equilibrium" measurement, is in fact determined by compressing a film of polymer at a fixed, slow rate (30 cm^2 min^{-1} typically). At high surface concentrations there is little resistance from the film to in-plane compression or dilation—compressing the film slowly in this region causes a surface "train" of polymer to loop into the subphase, and dilating the film causes a loop of polymer to adsorb to the surface, maintaining the "saturated" surface concentration. This desorption/adsorption can occur during the time scale of the film compression, hence the low elasticity measured. On the other hand, in the case of the SQELS measurement, the time scale of the determination of the modulus is much shorter ($\sim 1/\omega_0$) since the surface is distorted by the capillary waves at high frequency ($\omega_0 \sim 35$ kHz) which may be too fast for desorption to occur.[16]

The dilational viscosity results are the most challenging, negative values being observed at all surface concentrations. Negative dilational viscosities have now been observed many times for various PEO-containing systems[12,13,18,37] and in some other cases.[35,38] Conventional thinking would regard a negative viscosity as unphysical since viscosities (whether bulk or surface) are associated with the dissipation of mechanical energy, and thus a negative viscosity implies energy being input from an external source. The dilational viscosity, to first order, increases the damping of the dilational waves by an amount $\Delta\Gamma_D$:[24]

$$\Delta\Gamma_D = \frac{2}{3}\left(\frac{\epsilon'^3\epsilon_0 q^8}{\eta^2\rho^{2-}}\right)^{1/3} \tag{13}$$

A negative dilational viscosity, therefore, means that the damping of the dilational waves is *less* than it would be if there was no dilational viscosity. This does *not* mean that the dilational waves have a negative damping; if that were the case, the surface oscillations would grow indefinitely. There is still a finite damping, but this damping is reduced from that given by eq 5b.

We are dealing with a system in thermodynamic equilibrium, so at first glance any explanation based on the concept of energy being fed into the dilational waves does not seem tenable. However, we only measure two of up to five possible surface motions,[3,4] and in fact we only directly detect one of those, the capillary waves; thus, it is possible that energy is being transferred into the dilational mode from one of the other surface modes. One such coupling is already well-known, between the capillary and dilational waves. Since energy transfer is a maximum at resonance, we would expect to see the dilational viscosity become more negative at the resonance between the capillary and dilational wave modes if the capillary modes were the source of the energy. At around the surface concentration of 0.4 mg m^{-2}, this does not seem to be the case.

An alternative explanation for the negative dilational viscosities is that the dispersion equation (eq 1) does not describe the observed surface oscillations completely. The implication is that at least one extra parameter is required in the "dilational" part of eq 1. This point is further discussed below.

Frequency Dependence. For this system we found little frequency dependence of the viscoelastic parameters determined by SQELS at the surface concentration of 0.4 mg m^{-2}. This is not surprising because we have estimated (Figure 12) for 0.4 mg m^{-2} a relaxation time of about 10^{-5} s, corresponding to $\omega_0 \sim 600$ kHz. Thus, to observe relaxation effects, we would have to take measurements at frequencies around 600 kHz, and such a capillary wave frequency is at present beyond the range of our apparatus, which currently has a maximum frequency of 320 kHz. However, we can use typical values obtained for the surface viscoelastic parameters to predict the frequency and damping of the capillary and dilational waves. These can then be compared with the experimentally observed frequency and damping for the capillary waves, as shown in Figure 13. The frequency and damping data have been normalized by the first-order approximations of eq 4 for pure water. This normalization factors out the approximate overall $q^{3/2}$ and q^2 variations of respectively the frequency and damping, allowing the differences between the measured and predicted capillary wave frequencies and dampings to be easily observed.

In Figure 13 the predicted normalized frequency is approximately 1.0, agreeing well with the measured normalized frequency. The prediction for the damping, however, is up to

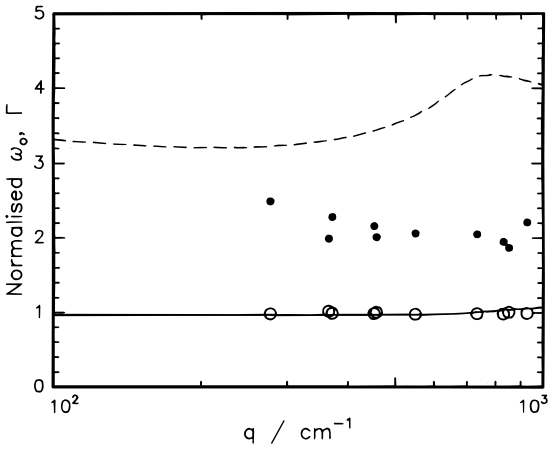

Figure 13. Normalized frequency (—, ○) and damping (- - -, ●). Lines are calculated from surface viscoelastic parameters and the dispersion equation, and points correspond to experimentally measured values.

twice the measured value. Such differences between the measured dampings and those predicted from the viscoelastic parameters returned by a spectral fit have been observed before.[24] It is worthwhile pointing out that such differences would not be noticed in data analysis methods which assume that $\gamma_0 = \gamma_{static}$, $\gamma' = 0$ and determine ϵ_0 and ϵ' from the measured frequency and damping. The lack of correspondence between the measured and predicted dampings may indicate that the dispersion equation does not describe the system adequately. We have already noted that the dilational viscosity is negative, an apparently unphysical result. We can hypothesize that what we currently assign to the dilational viscosity is in fact a combination of the true dilational viscosity and some extra (as yet unknown) parameter in the dilational part of the dispersion equation (eq 1).

Comparison with Linear PEO. SQELS data for linear PEO ($M_w = 15\,000$) have been reported earlier.[12] Comparing data obtained at approximately the same wave vector, q, there are clear differences. At surface concentrations greater than 0.6 mg m^{-2}, the dilational modulus and dilational viscosity of the linear polymer abruptly fall, at the same time the transverse shear viscosity rises. None of this behavior is observed for the cyclic polymer

The most obvious difference between linear and cyclic polymers is that the former has two free ends possibly with end groups that differ chemically from the rest of the polymer. As well as processes driven by chemically different end groups (e.g., surface enrichment) linear polymers can, if in a melt or sufficiently concentrated solution and above a critical molecular weight, entangle whereas a cyclic polymer cannot. A 2-D overlap concentration can be defined as $c^* \approx 1/\pi R_g^2$. For the 15 K polymer, $R_g \approx 6.5$ nm and so $c^* \approx 7.5 \times 10^{-3}$ chains nm^{-2}, corresponding to a surface concentration of $\Gamma_s \approx 0.2$ mg m^{-2}. So across the range of surface concentrations studied, the linear PEO previously studied was in this overlap region. The coincidence of the SQELS data for linear and cyclic PEO below 0.6 mg m^{-2} indicates that entanglements and chain ends do not affect the surface behavior of chains at low surface concentrations for the capillary wave frequencies studied. Above 0.6 mg m^{-2}, where the linear and cyclic PEO significantly penetrate the subphase, the differences observed in the surface viscoelastic parameters may be due to the presence of free ends in the linear polymer.

Conclusions

Surface quasielastic light scattering has been used to investigate the surface viscoelasticity of spread films of cyclic poly(ethylene oxide) at various surface concentrations of polymer. We have shown that increasing the surface concentration of polymer causes complex variations in the capillary wave frequency and damping which can only be explained by the existence of a resonance between the capillary and dilational waves. Further analysis of the raw data in terms of four surface viscoelastic parameters—surface tension, transverse shear viscosity, dilational modulus, and dilational viscosity—has demonstrated a change in the dynamic behavior of the surface as the polymer film is compressed and the surface concentration increases. At surface concentrations below 0.4 mg m^{-2}, the surface tensions and dilational moduli measured at capillary wave frequencies are the same as the static values. Well above this surface concentration at least one relaxation occurs in the frequency regime studied. For the (in-plane) dilational mode this relaxation is associated with the rate of desorption of polymer chains from the interface into the subphase when the surface is saturated with polymer.

To fit the data adequately, two surface viscosities have to be included in the model dispersion equation: transverse shear viscosity and dilational viscosity. The transverse shear viscosity increases at higher surface concentrations due to increased concentration of chains in the immediate subsurface; however, below 0.4 mg m^{-2} this viscosity is anomalous—decreasing with increasing surface concentration. The apparently unphysical measurement of negative dilational viscosities at all surface concentrations has been rationalized as a reduction in the damping of the dilational waves below that expected for a film with $\epsilon' = 0$. This may have two origins: either a coupling with another surface oscillation mode or because the dispersion equation does not describe the surface behavior completely. This latter conclusion is supported by the fact that there is a discrepancy between the capillary wave damping calculated from the observed surface viscoelastic parameters and that measured directly.

Acknowledgment. Thanks are due to EPSRC for the financial support of the research projects of which this work forms a part. We are also grateful to Prof. John Earnshaw of Queen's University, Belfast, for the kind provision of fitting algorithms and his continuing encouragement of our work.

References and Notes

(1) Fleer, G. J.; Cohen-Stuart, M. A.; Scheutjens, J. M. H. M.; Cosgrove, T.; Vincent, B. *Polymers at Interfaces*; Chapman and Hall: London, 1993.
(2) Langevin, D. *Light Scattering by Liquid Surfaces and Complementary Techniques*; Marcel Decker: New York, 1992; Vol. 41.
(3) Goodrich, F. C. *J. Phys. Chem.* **1962**, *66*, 1858.
(4) Goodrich, F. C. *Proc. R. Soc. London A* **1981**, *374*, 341.
(5) Hard, S.; Hamnerius, Y.; Nilsson, O. *J. Appl. Phys.* **1976**, *47*, 2433.
(6) Earnshaw, J. C.; McGivern, R. C. *J. Colloid Interface Sci.* **1988**, *123*, 36.
(7) Winch, P. J.; Earnshaw, J. C. *J. Phys. E: Sci. Instrum.* **1988**, *21*, 287.
(8) Earnshaw, J. C.; McGivern, R. C.; McLaughlin, A. C.; Winch, P. J. *Langmuir* **1990**, *6*, 649.
(9) Bjorkvik, B. J. A.; Waaler, D.; Sikkeland, T.; Strand, K. A.; Stromme, G. *Meas. Sci. Technol.* **1995**, *6*, 1572.
(10) Cao, B. H.; Kim, M. W. *Faraday Discuss.* **1994**, *98*, 245.
(11) Henderson, J. A.; Richards, R. W.; Penfold, J.; Thomas, R. K.; Lu, J. R. *Macromolecules* **1993**, *26*, 4591.
(12) Richards, R. W.; Taylor, M. R. *J. Chem. Soc., Faraday Trans.* **1996**, *92*, 601.
(13) Peace, S. K.; Richards, R. W.; Williams, N. *Langmuir* **1988**, *14*, 667.

(14) Richards, R. W.; Rochford, B. R.; Taylor, M. R. *Macromolecules* **1996**, *29*, 1980.
(15) Richards, R. W.; Peace, S. K. *Polymer* **1996**, *37*, 4945.
(16) Sauer, B. B.; Yu, H. *Macromolecules* **1989**, *22*, 786.
(17) Kawaguchi, M.; Sauer, B. B.; Yu, H. *Macromolecules* **1989**, *22*, 1735.
(18) Huang, Q. R.; Wang, C. H. *Langmuir* **1996**, *12*, 2679.
(19) Cao, B. H.; Kim, M. W.; Cummings, H. Z. *J. Chem. Phys.* **1995**, *102*, 9375.
(20) Cao, B. H.; Kim, M. W. *Europhys. Lett.* **1995**, *29*, 555.
(21) Yan, Z.-G.; Yang, Z.; Price, C.; Booth, C. *Makromol. Chem. Rapid Commun.* **1993**, *14*, 725.
(22) Yu, G. E.; Sinnathamby, P.; Price, C.; Booth, C. *Chem. Commun.* **1996**, 31.
(23) Earnshaw, J. C.; McLaughlin, A. C. *Proc. R. Soc. London, Ser. A* **1991**, *433*, 663.
(24) Earnshaw, J. C.; McLaughlin, A. C. *Proc. R. Soc. London A* **1993**, *440*, 519.
(25) Langevin, D.; Meunier, J.; Chatenay, D. In *Surfactants in Solution;* Langevin, D., Meunier, J., Chatenay, D., Eds.; Plenum: New York, 1984; Vol. 3, pp 1991.
(26) Griffiths, P. C.; Stilbs, P.; Yu, G. E.; Booth, C. *J. Phys. Chem.* **1995**, *99*, 16752.
(27) Cooke, J.; Yu, G. E.; Sun, T.; Yonemitsu, T.; Viras, K.; Gorry, P. A.; Ryan, A. J.; Price, C.; Booth, C. *Macromolecules*, submitted for publication.
(28) Malvern K7025. Malvern Instruments, Spring Lane, Malvern WR14 1AQ, UK.
(29) Model 601A. Nima Technology Ltd, The Science Park, Conventry, CV4 7EZ, UK.
(30) Birecki, H.; Amer, N. M. *J. Phys. (Paris)* **1979**, *40*, c3.
(31) Lucassen-Reynders, E. H.; Lucassen, J. *Adv. Colloid Interface Sci.* **1969**, *2*, 347.
(32) Earnshaw, J. C.; Hughes, C. J. *Langmuir* **1991**, *7*, 2419.
(33) Crawford, G. E.; Earnshaw, J. C. *Biophys. J.* **1987**, *52*, 87.
(34) Earnshaw, J. C.; McGivern, R. C.; Winch, P. J. *J. Phys.* **1988**, *49*, 1271.
(35) Earnshaw, J. C.; Sharpe, D. J. *J. Chem. Soc., Faraday Trans.* **1996**, *92*, 611.
(36) Adamson, A. W. *Physical Chemistry of Surfaces*, 5th ed.; Wiley-Interscience: New York, 1990.
(37) Richards, R. W.; Taylor, M. R. *Macromolecules* **1997**, *30*, 3892.
(38) Earnshaw, J. C.; McLaughlin, A. C. *Prog. Colloid Polym. Sci.* **1989**, *79*, 155.